

experiment the particles decayed while in air, the Weinstein¹² explanation would require the reaction $\tau \rightarrow \theta$ to have a cross section over 300 times geometrical for K mesons of velocity $\beta = 0.59$ in air. The cascade scheme of Lee and Orear,¹⁵ which still lacks any experimental verification, becomes less reasonable as the $\tau - \theta$ mass difference becomes smaller. Lee and Yang¹⁶ have recently proposed that there may be only one heavy meson of a certain spin and parity, but that its parity is not conserved when it decays. They point out

that one can postulate nonconservation of parity for all weak interactions without contradicting experiment.

We wish to thank Dr. E. J. Lofgren and members of the Radiation Laboratory staff of the University of California for their help in obtaining the Bevatron exposures. We are grateful to Mrs. J. Bielk, Mrs. E. Bierman, Mrs. J. Impeduglia, Mrs. M. Johnson, Mr. B. Kuharetz, and Miss J. Lee of the Columbia Nuclear Emulsion Group for their help with the scanning, processing, and measuring.

Inelastic and Elastic Scattering of 187-Mev Electrons from Selected Even-Even Nuclei*

RICHARD H. HELM†

High-Energy Physics Laboratory, Stanford University, Stanford, California

(Received August 27, 1956)

A survey has been made of the differential scattering cross sections for 187-Mev electrons on the even-even nuclei $^{12}\text{Mg}^{24}$, $^{14}\text{Si}^{28}$, $^{16}\text{S}^{32}$, $^{18}\text{A}^{40}$, and $^{88}\text{Sr}^{88}$. It has been possible to separate the elastic scattering from the inelastic in all cases and to resolve the inelastic groups from specific nuclear levels for at least one level in all cases. A simple Born-approximation analysis of the elastic data yields values of the effective radii and surface thicknesses of the nuclear charge densities which (if suitably corrected for failure of the Born approximation) are in substantial agreement with the results of Hahn, Ravenhall, and Hofstadter; i.e., a radius parameter of $c \approx 1.08 \text{ } A^{\frac{1}{3}} \times 10^{-13} \text{ cm}$ (radius to half-maximum of the charge distribution) and a surface thickness of $t \approx 2.5 \times 10^{-13} \text{ cm}$ (thickness from 10% to 90% of the maximum of the charge distribution). Phenomenological analysis of the inelastic scattering along the lines laid down by Schiff yields some tentative multipolarity assignments, and application of some results of Ravenhall yields estimates of (radiative) partial level widths; for the $E2$ transitions these correspond to lifetimes of $\sim 19 \times 10^{-13} \text{ sec}$ ($\text{Mg } 1.37 \text{ Mev}$) to $\sim 1.4 \times 10^{-13} \text{ sec}$ ($\text{Sr } 1.85 \text{ Mev}$). The observed strengths of the transitions are compared to those predicted by Weisskopf theory.

I. INTRODUCTION

THE elastic scattering of high-energy electrons by atomic nuclei has been the subject of considerable experimental study.¹⁻⁸ Recently it has been possible in this laboratory to observe certain examples of inelastic scattering⁹⁻¹¹ in which the incident high-energy electron is scattered with the loss of a discrete quantum of energy corresponding to the excitation of a level in the target nucleus.

* The research reported in this document was supported jointly by the U. S. Navy (Office of Naval Research) and the U. S. Atomic Energy Commission, and by the U. S. Air Force through the Air Force Office of Scientific Research, Air Research and Development Command.

† Now at the University of California Los Alamos Scientific Laboratory, Los Alamos, New Mexico.

¹ Hanson, Lyman, and Scott, Phys. Rev. **84**, 626, 638 (1951).

² H. R. Fechter (unpublished).

³ Hofstadter, Fechter, and McIntyre, Phys. Rev. **91**, 422 (1953).

⁴ Hofstadter, Fechter, and McIntyre, Phys. Rev. **92**, 978 (1953).

⁵ Hofstadter, Hahn, Knudsen, and McIntyre, Phys. Rev. **95**, 512 (1954).

⁶ R. Hofstadter and R. W. McAllister, Phys. Rev. **98**, 217 (1955).

⁷ R. W. Pidd and C. L. Hammer, Phys. Rev. **99**, 1396 (1955).

⁸ Hahn, Ravenhall, and Hofstadter, Phys. Rev. **101**, 1131 (1956).

⁹ McIntyre, Hahn, and Hofstadter, Phys. Rev. **94**, 1084 (1954).

¹⁰ J. A. McIntyre and R. Hofstadter, Phys. Rev. **98**, 158 (1955).

¹¹ J. H. Fregeau and R. Hofstadter, Phys. Rev. **99**, 1503 (1955).

The present experiments were initiated as a survey of the inelastic and elastic scattering from even-even nuclei in the region of intermediate atomic numbers. These target materials were chosen for a number of reasons: First, most of them are known from gamma-ray spectroscopy, angular correlations, etc., to have easily excited low-lying levels with spacings on the order of a few Mev, which should be resolvable in an experiment of the type of Fregeau and Hofstadter.¹¹ Second, the principal isotope of most of these elements occurs in high abundance, so that the natural form may be used in the targets. Third, the ground state has zero spin and even parity in the known cases (see, e.g., Endt and Kluyver¹² and probably in all cases (i.e., from shell-structure arguments); furthermore, it usually happens¹²⁻¹⁴ that one or more of the lower levels has known total angular momentum and a parity consistent with electric-type multipole transitions from the ground state. This last point is important because the

¹² P. M. Endt and J. C. Kluyver, Revs. Modern Phys. **26**, 94 (1954).

¹³ F. Ajzenberg and T. Lauritsen, Revs. Modern Phys. **24**, 321 (1952).

¹⁴ B. B. Kinsey and G. A. Bartholomew, Can. J. Phys. **31**, 1051 (1953); G. R. Bishop and J. P. Perez y Jorba, Phys. Rev. **98**, 89 (1955).

electric transitions should be particularly easily interpreted theoretically,^{15,16} at least phenomenologically, and therefore should be valuable in checking the theory.

While this work was intended primarily to be a preliminary survey, it was anticipated that considerable information could be derived from the results. The elastic-scattering angular distribution should give information as to the radial dependence of the nuclear charge distributions.^{3-5,8,17-23} The inelastic cross sections, if measured accurately enough over wide enough ranges of scattering angle and energy of the incident electrons, should enable one (a) to determine the multipolarity and electric or magnetic character of the transitions²⁴ which will supplement γ - and β -ray work and Coulomb excitation in assigning angular momentum and parity to the various states; (b) to determine the magnitude and shape of the transition charge density and hence obtain considerable information about the various wave functions; (c) to derive a number of interesting parameters such as the transition probabilities (or level widths). Such a complete analysis is beyond the scope of the present work. However, it has been possible to decide with fair certainty that several observed transitions are electric monopole, quadrupole, or octupole where this was not previously known, and to estimate the transition probability and certain gross features of the transition charge density in the known electric-quadrupole cases.

II. EXPERIMENTAL METHOD

The experiments were performed at the first halfway station of the Stanford Mark III linear accelerator, using the magnetically analyzed and deflected electron beam and the 16-in. magnetic spectrometer. The accelerator,²⁵ and the spectrometer and its associated counting and beam monitoring equipment including a number of recent improvements are described in earlier articles.^{2-6,8-11}

The important physical properties of the various targets are summarized in Table I. With the exception

TABLE I. Target parameters.

Element	Mass No.	Principal isotope	Percent abundance	Target thickness, gross			$10^{-22} \times \text{No. atoms/cm}^2$	$10^{-22} \times \text{No. atoms/cm}^2$	$10^{-22} \times \text{No. atoms/cm}^2$
				Inches	g/cm ²	Radiation lengths			
¹² Mg ²⁴	24	78.8	0.13	0.570	1.93×10^{-2}	1.42	1.12		
¹⁴ Si ²⁸	28	92.2	0.70	0.41	1.62×10^{-2}	0.885	0.816		
¹⁶ S ³²	32	95.0	0.118	0.588	2.64×10^{-2}	1.11	1.05		
³⁸ Sr ⁸⁸	88	82.7	0.050	0.33	2.94×10^{-2}	0.23	0.19		
¹⁸ A ⁴⁰	40	99.6	...	0.66	5.96×10^{-2}	0.46	0.38		
CH ₂	1	14.3	0.119	0.275	0.55×10^{-2}	2.38	

of the argon, which was used in a high-pressure gas target chamber,²⁶ all the targets were in the form of wafers, roughly 1 in. by 2 in. in size. Surface densities were found by weighing and measuring with a precision of a few percent; the uncertainty in the Si target thickness was slightly greater, possibly 5% because of visible pits in the material. The CH₂ (polyethylene) target was used for an "absolute" cross-section calibration in the manner described by Fregeau and Hofstadter.¹¹

The spectra of electrons scattered at various angles were taken as described in previous publications.^{2-6,8-11} Typical spectrometer curves are shown in Fig. 1. They are seen to be characterized by an elastic peak and one or more resolved or partially resolved inelastic peaks, shifted downward from the elastic peak by the characteristic excitation energies of the corresponding nuclear levels. The widths of the peaks (i.e., with at half-maximum) are well explained by the combined effects of beam energy spread, spectrometer resolution setting, beam size, and ionization straggling in the target; however, while the fold of these effects is an essentially Gaussian shape, the observed peaks are broader at the base than is a Gaussian (probably because of scattering from the spectrometer vacuum chamber, exit port, etc.) and have a long, low-energy tail resulting from radiation processes in the target. In subtracting the tail of the elastic peak from the inelastic peaks it usually has been sufficient to fit an empirical tail of the form $A(E_0-E)^{-1} + B(E_0-E)^{-2}$ and to adjust the parameters until the various peaks of a given spectrometer curve have the same shape after the subtraction.

In principle, the relative intensities of the peaks should be subject to a number of corrections: (1) correction for isotopic abundance, since all isotopes will contribute to the elastic peak but only the principal isotope will contribute to the inelastic peaks; (2) the variation of spectrometer "window width" with energy setting should be taken into account (i.e., $\Delta E \sim E$); (3) the effects of finite resolution in angle ($\sim \pm 1.8^\circ$) and energy (0.5–1.0 Mev) on the angular distributions; (4) effects of plural scattering (the $n=2,3,\dots$ terms in

¹⁵ L. I. Schiff, Phys. Rev. **96**, 765 (1954).

¹⁶ C. J. Mullin and E. Guth, Phys. Rev. **98**, 277(A) (1955).

¹⁷ E. Guth, Anz. Akad. Wiss. Wien, Math.-naturw. Kl. **24**, 299 (1934); Thie, Mullin, and Guth, Phys. Rev. **87**, 962 (1952).

¹⁸ M. E. Rose, Phys. Rev. **73**, 279 (1948).

¹⁹ J. H. Smith, Cornell University, Ph.D. thesis, 1951 (unpublished).

²⁰ L. R. B. Elton, Proc. Phys. Soc. (London) **A63**, 1115 (1950); **A65**, 481 (1952); Phys. Rev. **79**, 412 (1950).

²¹ Yennie, Ravenhall, and Wilson, Phys. Rev. **95**, 500 (1954).

²² L. I. Schiff, Phys. Rev. **92**, 988 (1953).

²³ G. E. Brown and L. R. B. Elton, Phil. Mag. **46**, 164 (1955).

²⁴ D. G. Ravenhall (to be published).

²⁵ R. B. Neal, Stanford University Microwave Laboratory Technical Report No. 185 (unpublished); Chodorow, Ginzton, Hansen, Kyhl, Neal, and Panofsky, Rev. Sci. Instr. **26**, 134 (1955); McIntyre, Kyhl, and Panofsky, Stanford University Microwave Laboratory Technical Report No. 202 (unpublished); W. K. H. Panofsky and J. A. McIntyre, Rev. Sci. Instr. **25**, 287 (1954); G. W. Tautfest and H. R. Fechter, Phys. Rev. **96**, 35 (1954).

²⁶ Hofstadter, McAllister, and Wiener, Phys. Rev. **96**, 854(A) (1954).

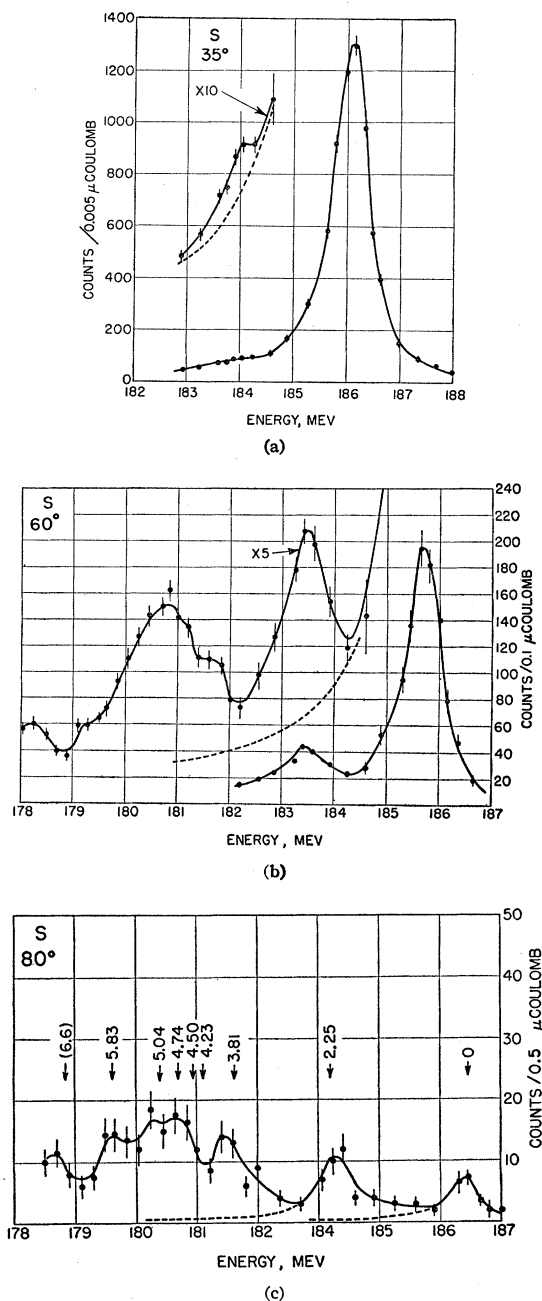


FIG. 1. Spectrometer curves: 187-Mev electrons on S.

the Molière²⁷ series); (5) corrections for Schwinger²⁸ and bremsstrahlung radiation. Effect (1) amounts to up to 26% (Mg). Effect (2) is generally negligible in view of the small shifts of inelastic peaks relative to the incident energy. Effect (3) estimated in the manner of Hanson, Lyman, and Scott¹ amounts to perhaps 5% in the region of the diffraction minima and has been

²⁷ G. Molière, Z. Naturforsch. 3a, 78 (1948).

²⁸ J. Schwinger, Phys. Rev. 75, 898 (1949); H. Suura, Phys. Rev. 99, 1020 (1955).

been ignored. Plural scattering (4) is estimated²⁹ to contribute <1% to the observed scattered intensities.

Of the radiation corrections (5), the Schwinger effect is estimated to decrease the observed intensity by ~8% at small angles to ~20% at large angles, and the bremsstrahlung in typical cases is estimated³⁰ to decrease the intensities by ~20% at small angles to ~40% at large angles. The radiation corrections have not been applied in analyzing the data, and the following remarks should be made: (a) the corrections vary slowly with angle and therefore will affect mainly the absolute cross sections; (b) the bremsstrahlung correction should be applied to both the "measured" and "calculated" cross sections (see Table II for explanation) but the "measured" cross sections already have been corrected for Schwinger effect (because the proton cross sections used in this calibration have been corrected) while the "calculated" cross section has not; (c) the main effect of ignoring the angular dependence of the radiation corrections will be a slight overestimate of the surface thickness parameters of the nuclear charge densities (see Secs. III, IV).

III. ANALYSIS OF ELASTIC DATA

It is convenient to analyze the scattering cross sections by means of the Born approximation.³¹ The exact calculations of Yennie, *et al.*²¹ show that although the Born approximation is considerably in error for high-energy electrons in medium-to-high atomic-numbered elements, it is probably still accurate enough to account for most of the important features of the scattering.

The Born approximation result, as used here, is given in terms of a nuclear form factor, F :

$$d\sigma/d\Omega = (d\sigma/d\Omega)_{\text{point}} |F|^2, \quad (1)$$

$$F(\mathbf{q}) = \int \rho(\mathbf{r}) e^{i\mathbf{q} \cdot \mathbf{r}} d^3\mathbf{r}. \quad (2)$$

Here $(d\sigma/d\Omega)_{\text{point}}$ is the differential scattering cross section of a point charge Ze ; \mathbf{q} is the momentum transfer of the electron in the scattering process; and $\rho(\mathbf{r})$ is the probability density of the charge distribution, normalized so that $\int \rho(\mathbf{r}) d^3\mathbf{r} = 1$.

For the point-charge cross section, it is not clear whether one should use the Born-approximation, or an exact calculation of the type made by Feshbach.³² As suggested by Schiff,²² the correct function may be something between these. In the present case, the

²⁹ H. A. Bethe and J. Ashkin, *Experimental Nuclear Physics*, edited by E. Segrè (John Wiley and Sons, Inc., New York, 1953), Vol. I, p. 290.

³⁰ Using the radiation straggling expressions given by W. Heitler, *The Quantum Theory of Radiation* (Clarendon Press, Oxford, 1954), third edition, p. 378.

³¹ For bibliography of Born approximation in electron scattering, see reference 22.

³² H. Feshbach, Phys. Rev. 88, 295 (1952).

TABLE II. "Calculated cross sections": experimental angular distributions, expressed in absolute units by fitting elastic data to cross sections calculated from the gU charge distributions (Sec. III).

Angle	¹² Mg ²⁴		¹⁴ Si ²⁸	
	Elastic	1.37 Mev	Elastic	1.78 Mev
40°	426 ± 14	22.2 ± 3.2	382 ± 11	6.5 ± 0.8
50°	74.5 ± 1.0	8.9 ± 1.3	61 ± 3	4.50 ± 0.60
60°	15.0 ± 0.5	3.9 ± 0.7	10.3 ± 0.2	2.39 ± 0.14
70°	1.61 ± 0.10	1.44 ± 0.11	1.13 ± 0.08	0.76 ± 0.08
80°	0.24 ± 0.02	0.52 ± 0.04	0.11 ± 0.02	0.24 ± 0.02
90°	0.065 ± 0.029	0.15 ± 0.03	0.012 ± 0.006	0.074 ± 0.012
100°	0.014 ± 0.003	0.042 ± 0.006
110°	0.0075 ± 0.0019	0.012 ± 0.002

Angle	¹² S ³²		¹⁴ S ³²	
	Elastic	2.25 Mev	3.81 Mev	5.83 Mev
35°	1250 ± 23	17 ± 3
40°	480 ± 15	10.3 ± 1.2	3.5 ± 1.2	4.1 ± 0.9
50°	69 ± 1.5	4.4 ± 0.4
60°	8.55 ± 0.35	1.22 ± 0.08	0.34 ± 0.05	0.27 ± 0.06
70°	0.81 ± 0.06	0.225 ± 0.032	0.17 ± 0.06	0.14 ± 0.06
80°	0.050 ± 0.007	0.083 ± 0.012	0.076 ± 0.024	0.059 ± 0.024
85°	0.060 ± 0.008	0.052 ± 0.008
90°	0.055 ± 0.005	0.026 ± 0.006	0.012 ± 0.006	0.028 ± 0.011
100°	0.040 ± 0.006	0.0079 ± 0.0024	0.006 ± 0.003	0.015 ± 0.005
110°	0.011 ± 0.003

Angle	¹² A ⁴⁰		¹⁴ A ⁴⁰	
	Elastic	1.46 Mev	2.4 Mev	...
50°	57	10.5 ± 1.9	1.6 ± 0.9	...
60°	5.9	1.4 ± 0.1	0.63 ± 0.08	...
70°	0.36	0.32 ± 0.07

Angle	¹² Sr ⁸⁸		¹⁴ Sr ⁸⁸	
	Elastic	1.85 Mev	2.76 Mev	4.3 Mev ^a
35°	2640 ± 100
40°	538 ± 16	17.2 ± 1.4	13.5 ± 1.3	3.7 ± 0.7
45°	158 ± 8
50°	35.7 ± 1.7	3.1 ± 0.4	5.1 ± 0.4	1.27 ± 0.24
55°	18.0 ± 1.1
60°	10.8 ± 0.5	0.41 ± 0.12	1.81 ± 0.13	0.74 ± 0.12
70°	5.0 ± 0.3	0.30 ± 0.11	0.53 ± 0.10	0.37 ± 0.10
80°	1.38 ± 0.10	0.11 ± 0.05	0.168 ± 0.048	0.12 ± 0.04

^a This level has not been reported previously, and may represent impurities (see Sec. VI).

choice is not critical, and the Feshbach results have been used (see Figs. 2 and 3).

In fitting the experimental data, it has proved convenient to use a "folded" charge distribution, given by

$$\rho(\mathbf{r}) = \int \rho_0(\mathbf{r}')\rho_1(\mathbf{r}-\mathbf{r}')d^3\mathbf{r}', \quad (3)$$

where

$$\int \rho(\mathbf{r})d^3\mathbf{r} = \int \rho_0(\mathbf{r})d^3\mathbf{r} = \int \rho_1(\mathbf{r})d^3\mathbf{r} = 1.$$

When (3) is substituted in (2), it follows that

$$F(\mathbf{q}) = F_0(\mathbf{q})F_1(\mathbf{q}), \quad (4)$$

where F_0 and F_1 result from the substitution of ρ_0 and ρ_1 , respectively, in Eq. (2). The advantage of this is that one can use trial functions of such a form that, for example, ρ_0 essentially defines the nuclear radius and ρ_1 a surface thickness; the resulting form factor is then

readily calculated for different ratios of the two parameters.

As is shown by Hahn *et al.*,⁸ the scattering at these energies depends mainly on the shape of the charge distribution near the surface and is relatively insensitive to the distribution at the center of the nucleus. Hence, it is sufficient to take for $\rho_0(r)$ a uniform distribution of radius $R \sim r_0 A^{1/3}$, where $r_0 \sim 1.2 \times 10^{-13}$ cm; it is then assumed that $\rho_1(r)$ is a (spherically symmetric) distribution of effective radius $\sim r_0$. The following two models will be considered:

$$\rho_0 = \begin{cases} 3/4\pi R^3, & r < R \\ 0, & r > R, \end{cases} \quad (5)$$

and

$$\rho_1(r) = (2\pi g^2)^{-1/2} \exp(-r^2/2g^2), \quad (6)$$

or

$$\rho_1(r) = \begin{cases} 3/4\pi u^3, & r < u \\ 0, & r > u, \end{cases} \quad (7)$$

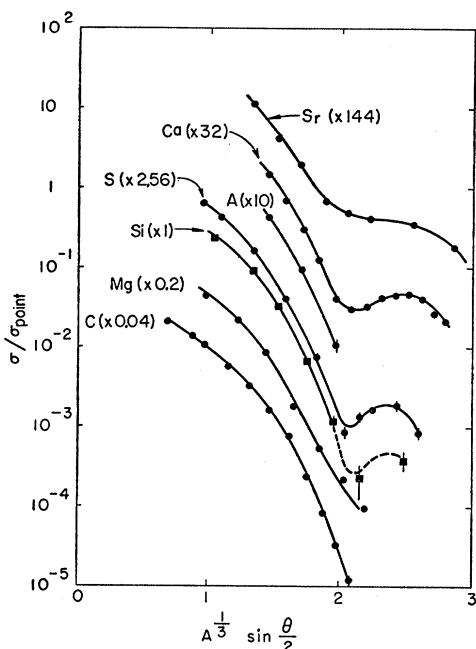


FIG. 2. Elastic angular distributions (observed cross sections divided by Feshbach point-charge cross sections). The results of Hahn *et al.* (reference 8) for Ca and of Fregeau and Hofstadter (reference 11) for C are included for comparison.

Substitutions of (5) and (6) in (3) will be termed a "Gaussian-uniform" or gU distribution, and substitution of (5) and (7) will be termed "uniform-uniform" or uU.

For comparison with other work, the rms radii will

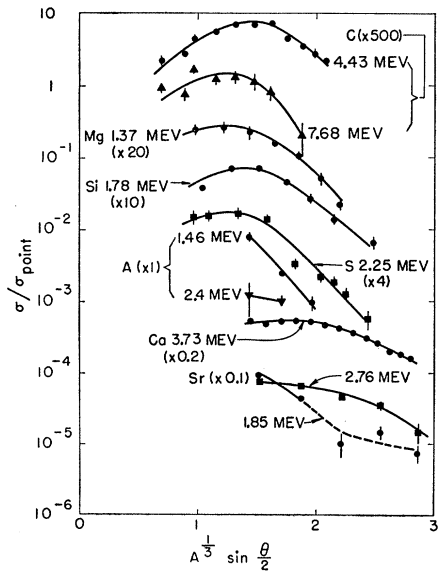


FIG. 3. Inelastic angular distributions (observed cross section divided by Feshbach point-charge cross sections). The results of Hahn *et al.* (reference 8) for Ca and of Fregeau and Hofstadter (reference 11) are included for comparison.

be calculated and expressed in terms of r_0^{33} :

$$r_0 = A^{-\frac{1}{3}} R_0,$$

$$R_0^2 = (5/3) \int r^2 \rho(r) d^3 r = (5/3) (\langle r^2 \rangle_0 + \langle r^2 \rangle_1), \quad (8)$$

where

$$\langle r^2 \rangle_{0,1} = \int r^2 \rho_{0,1}(r) d^3 r.$$

It is known from the work of Yennie *et al.*²¹ that, while the Born approximation fails completely in the region of the zeros predicted by discontinuous distributions such as (5), it is quite accurate for values of $qR < 90\%$ of its value at the first zero, and again in the region midway between the successive zeros.

The data-fitting procedure which has been adopted consists of choosing several values of R , and for each one picking the value of R/g or R/u which best fits the calculated $|F|^2$ to the experimental $|F|^2$. Because the data are rather scanty and because the Born approximation is not very accurate, least-square fits were not attempted; the best fits were chosen by inspection. It is felt that the subjective bias introduced by this procedure is at least qualitatively unimportant in showing how the parameters vary from element to element. Typical "best fits" of the form factors of two charge distributions to the data are shown in Fig. 4.

IV. RESULTS: ELASTIC DATA

(The data of Hahn, *et al.*⁸ for calcium and of Fregeau and Hofstadter¹¹ for carbon are included for purposes of comparison.) It is seen from Table III that the radial- and surface-thickness parameters differ appreciably with choice of model but are quite constant as a function of A and Z for a given model. Thus, for the gU model, $r_0 \approx (1.35 \pm 0.04) \times 10^{-13}$ cm, and $g \approx (1.0 \pm 0.1) \times 10^{-13}$ cm for all elements investigated; for the uU model, $r_0 \approx (1.32 \pm 0.04) \times 10^{-13}$ cm and $u \approx (2.0 \pm 0.3) \times 10^{-13}$ cm. The variations of the surface-thickness parameter from element to element (Table III), are greater than the estimated errors, have roughly the same form for both models, and may be real. The rms radius possibly varies slowly with A and Z but the variation is smooth within the estimated experimental accuracy. It should be noted, of course, that any smooth variation of the parameters with Z and A may be related to the worsening of the Born approximation in heavier nuclei.

It is interesting to note the remarkable agreement between the two models for the values of the parameters r_1 and t (see Table IV). Hahn *et al.*⁸ also noticed that these parameters are nearly independent of the model used.

Some insight as to the validity of using the Born

³³ This definition is equivalent to the r_0 of Hahn *et al.*, reference 8.

approximation to derive these parameters can be gained by comparison with the exact calculations of Hahn *et al.*⁸ Note that the Fermi smoothed-uniform shape

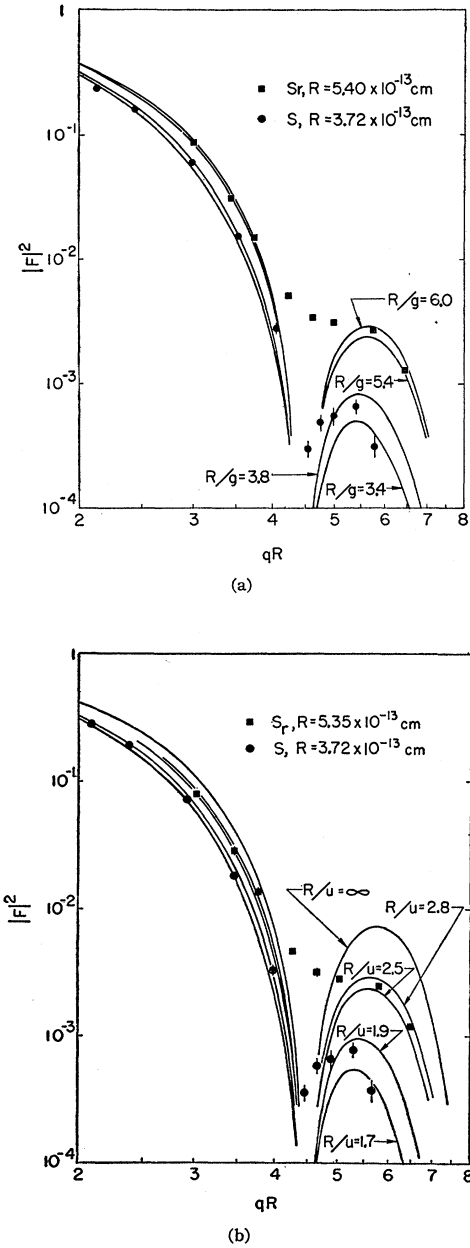


FIG. 4. Typical "best fits" of squared experimental form factors to calculated squared form factors, showing how a variation of 5–10% of the surface-thickness parameter from its "best" value gives noticeably worse fits. Variation of the radial parameter R by 2–3% either way also makes the fit worse for all choices of the surface-thickness parameter.

used by Hahn *et al.* somewhat resembles the models used in the present analysis. Thus for calcium, using the scattering data of Hahn *et al.*,

TABLE III. Parameters for gU and uU charge distributions.

Element	$A^{-1/3}R$	g	r_0	r_1	t	Corrected for Born approximation ^a		
						r_0	r_1	t
C ¹²	1.10	0.90	1.39	0.97	2.3	1.35	0.95	2.2
Mg ²⁴	1.14	1.03	1.39	1.03	2.7	1.33	0.99	2.6
Si ²⁸	1.12	1.07	1.35	1.01	2.9	1.29	0.97	2.8
S ³²	1.17	1.01	1.37	1.08	2.7	1.30	1.03	2.6
Ca ⁴⁰	1.20	0.93	1.85	1.14	2.5	1.28	1.08	2.4
Sr ⁸⁸	1.20	0.95	1.30	1.17	2.5	1.20	1.08	2.3

Element	$A^{-1/3}R$	u	r_0	r_1	t	Corrected for Born approximation ^a		
						r_0	r_1	t
C ¹²	1.11	1.7	1.33	0.96	2.1	1.29	0.93	2.0
Mg ²⁴	1.13	2.3	1.35	0.97	2.85	1.30	0.93	2.0
Si ²⁸	1.14	2.2	1.35	1.03	2.7	1.29	0.99	2.6
S ³²	1.17	2.1	1.34	1.08	2.6	1.28	1.03	2.5
Ca ⁴⁰	1.20	2.0	1.34	1.14	2.5	1.27	1.08	2.4
Sr ⁸⁸	1.20	2.0(5)	1.28	1.15	2.4	1.18	1.06	2.3

^a Correction factor $[1 + (3\alpha/2kR)]^{-1}$; see Sec. IV.

(i) gU and uU model (Born approximation):

$$\begin{aligned} r_1 &= (1.14 \pm 0.02) \times 10^{-13} \text{ cm}, \\ t &= (2.5 \pm 0.1) \times 10^{-13} \text{ cm}; \end{aligned}$$

(ii) Fermi smoothed-uniform (exact calculation)⁸:

$$\begin{aligned} r_1 &= (1.06 \pm 0.02) \times 10^{-13} \text{ cm}, \\ t &= (2.5 \pm 0.1) \times 10^{-13} \text{ cm}. \end{aligned}$$

The greater-than-probable difference in r_1 may be due in part to the use of different models, but probably also is related to the use of the Born approximation, which, because its neglects the modifications of the incident plane wave by the attractive potential of the nucleus, tends to give slightly larger values of the nuclear radii than do exact calculations. An estimate of this effect based on a uniform charge distribution shows

TABLE IV. Parameters associated with inelastic scattering. Indicated errors in β_i have been estimated roughly in fitting calculated squared form factors to the data (see Sec. V). Relative errors of Γ , τ and $|M|^2$ are roughly the same as for β_i . See Sec. V for definitions.

Element	Energy Mev	J_i parity	$\beta_i(I_i, I_f)$	$\Gamma_i(I_f \rightarrow I_i)$ millivolts	τ_i seconds	$ M ^2$
C ¹²	4.43	2+	0.40 ± 0.08	12.5	0.53×10^{-13}	2.3
Mg ²⁴	1.37	2+	0.34 ± 0.03	0.34	19×10^{-13}	9.1
Si ²⁸	1.78	2+	0.18 ± 0.03	1.1	6.0×10^{-13}	6.1
S ³²	2.25	(2+) ^a	0.11 ± 0.01	4.0	1.6×10^{-13}	5.8
A ⁴⁰	2.4	(2+) ^b	0.025 ± 0.005	2.0	3.3×10^{-13}	1.8
Ca ⁴⁰	3.73	(3-) ^a	0.125 ± 0.005	0.0093	0.71×10^{-10}	7.7
Sr ⁸⁸	1.85	2+	0.014 ± 0.001	4.7	1.4×10^{-13}	4.6
Sr ⁸⁸	2.76	3-	0.033 ± 0.003	0.0061	1.08×10^{-10}	7.1

^a Probable.

^b Assumed.

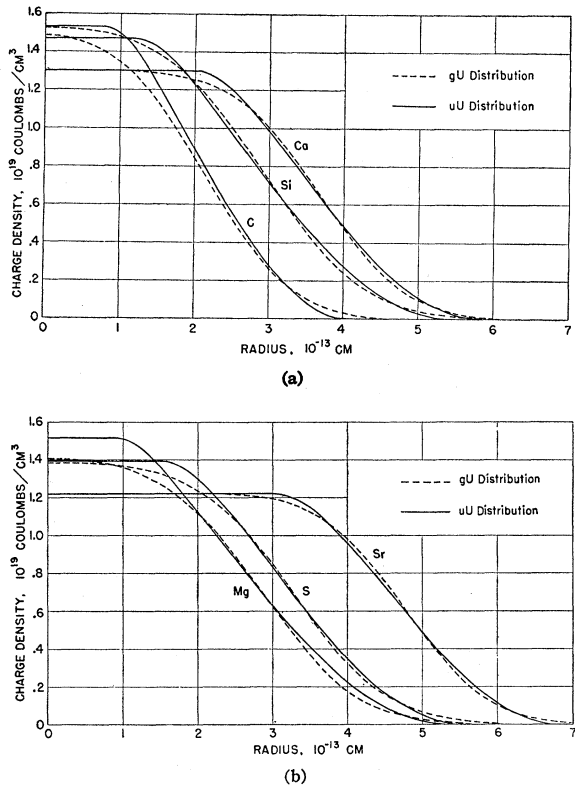


FIG. 5. Charge distributions calculated for the parameters given in Table III. The radius and surface-thickness parameters have been corrected by the factor $(1+3Z\alpha/2kR)^{-1}$.

that the Born-approximation radii should be reduced by the factor $[1+(3Z\alpha/2kR)]^{-1}$; for calcium in the present experiment this amounts to a 6% correction, giving r_1 (corrected) = 1.08×10^{-13} cm, in excellent agreement with Hahn *et al.* Figure 5 shows the charge distributions defined by the parameters of Table III.

It will be noticed that the conversion factors from "calculated" to "measured" cross sections, given in Table II, differ considerably from unity, ranging up to a factor of 2 for Sr. This discrepancy probably is due partly to some undetected experimental error in one of the hydrogen calibration points (Sec. II); it is possible also that using the Feshbach rather than the Born-approximation point-charge cross section was the wrong choice. (Thus the Feshbach point-charge cross section for Sr is 40% larger than the Born approximation, which could account for nearly half the discrepancy.) This error, although it seriously affects the magnitude of the absolute cross sections, will have little effect on the radius and surface-thickness parameters.

V. ANALYSIS OF INELASTIC DATA

The inelastic cross sections also may be discussed in terms of Born-approximation form factors, at least in the case of electric-multipole transitions. As is shown by

Schiff,¹⁵ Eq. (1) again holds in these cases, if the inelastic form factor is properly defined.

Writing out the general form of Eq. (25) of reference 15, the form factor for inelastic scattering involving an electric l -pole transition between an initial nuclear state I_i and a final state I_f is given by

$$\begin{aligned} |F_l(I_i, I_f)|^2 &= \frac{4\pi(2l+1)}{2I_i+1} \sum_{m_i, m_f} \\ &\times \left| \int j_l(qr) Y_{lm_i}(I_i, m_i; I_f, m_f) d^3 r \right|^2 \\ &= \beta_l(I_i, I_f) \left| 4\pi \int j_l(qr) \rho_l^{i,f}(r) r^2 dr \right|^2 \\ &= \beta_l(I_i, I_f) |f_l^{i,f}|^2 \end{aligned} \quad (9)$$

where

$$f_l^{i,f}(q) = 4\pi \int j_l(qr) \rho_l^{i,f}(r) r^2 dr; \quad (10)$$

here $\rho_l(I_i, m_i; I_f, m_f)$ is the transition matrix element between the initial and final states. The second equality holds because all the ρ_l are assumed to have the same radial dependence, so that the radial integral may be factored out. The quantity $\beta_l(I_i, I_f)$, then, brings together all the terms of the summations over nuclear orientation and in general will depend strongly on the details of the nuclear model. For the treatment that follows, the normalization of $\rho_l^{i,f}(r)$ will be unimportant, but will be taken arbitrarily so that $\langle r^l \rangle_{i,f} = R^l$ [see Eq. (12) below].

Now if we made an assumption as to the form of $\rho_l^{i,f}(r)$, and evaluate the integral in Eq. (10), and if we already know l or can infer it from the experimental shape of F_l then we can evaluate $\beta_l(I_i, I_f)$ by comparing $f_l^{i,f}$ with the experimental form factors. We may relate $\beta_l(I_i, I_f)$ to the width of the inverse γ -ray transition in the following way:

Expanding the Bessel function for small values of q , we obtain

$$|F_l(I_i, I_f)|^2_{q \rightarrow 0} = \beta_l(I_i, I_f) q^{2l} \left[\frac{\langle r^l \rangle_{i,f}}{1 \cdot 3 \cdots (2l+1)} \right]^2, \quad (11)$$

where

$$\langle r^l \rangle_{i,f} = 4\pi \int r^l \rho_l^{i,f}(r) r^2 dr. \quad (12)$$

This may be combined with an expression given for the γ -transition width by Ravenhall,²⁴ giving

$$\begin{aligned} \Gamma_l(I_f \rightarrow I_i) &= \frac{2I_i+1}{2I_f+1} \frac{\beta_l(I_i, I_f)}{[1 \cdot 3 \cdots (2l+1)]^2} \\ &\times 4Z^2 k^{2l} \langle r^l \rangle_{i,f}^2 \frac{e^2}{hc} \frac{l+1}{2l} \left(\frac{\epsilon}{E} \right)^{2l} \epsilon, \end{aligned} \quad (13)$$

where ϵ is the transition energy. It will be noticed that in the special case of $I_i = I_f = 0$, $l = 0$, Eqs. (9) and (10) should be replaced by

$$|F(0,0)|^2_{q \rightarrow 0} = \beta(0,0)[q^2 r_{0,0}^2 / 3]^2 \quad (14)$$

$$\langle r^2 \rangle_{0,0} = 4\pi \int r^2 \rho_{0,0}(r) r^2 dr. \quad (15)$$

This is because orthogonality of the excited- and ground-state wave functions requires that $4\pi \int \rho_{0,0}(r) r^2 dr = 0$.¹⁵ Also, Eq. (13) does not apply, but should be replaced by expressions for $\Gamma_{i.c.}$ and $\Gamma_{i.p.}$, the internal-conversion and internal-pair transition widths.

Following the suggestion of Bohr and Mottleson³⁴ and of Schiff,¹⁶ it will be assumed tentatively that a trial function for $\rho_l^{i,f}(r)$ may be taken as a delta function $\delta(r - R_l)$ when $l \neq 0$. When this is done, it may be seen (Fig. 6) that R_l must be some 20–30% larger than the value of R obtained for the static charge from the elastic data. However, if one smears out the delta function by the folding technique of Eq. (13) using the value of the parameter g or u [Eqs. (6) and (7)] found from the elastic data, then one finds that R_l (at least in the electric-quadrupole case) can be taken as equal to R .

In this connection it should be pointed out that Eq. (14) applies whether or not the $\rho(r)$ are spherically symmetric. Thus, if we assume $\rho_1(r)$, and, hence, $F_1(q)$ to be spherically symmetric, then the l th term of a multipole expansion of (r) will have the same form as the F_l in (9) with an additional factor $F_k(q)$:

$$|F_l(I_i, I_f)|^2 = \beta_l(I_i, I_f) \left| 4\pi \int j_l(qr) \rho_l^{i,f}(r) r^2 dr \right|^2 |F_1(q)|^2. \quad (16)$$

Equations (12) through (15) will be unchanged because $\lim_{q \rightarrow 0} [F_1(q)]^2 = \int \rho_1(r) d^3r = 1$.

In interpreting the results, it is useful to compare the experimental inelastic form factors to the functional form of Eq. (16). This has been done in Fig. 6.

It is of some interest to compare the predictions of the Weisskopf³⁵ single-particle model to the present results. Here the Weisskopf³⁵ wave functions for all states of the excited nucleon are taken to be constant out to radius R_w , and zero from R_w to infinity. Then, using the results of Ravenhall²⁴ for the inelastic-scattering cross section for the single-particle model, it follows that

$$|M|^2 = \left[\frac{(d\sigma/d\Omega)_{i,f}}{(d\sigma/d\Omega)_{\text{Weisskopf}}} \right]_{q \rightarrow 0} = \frac{\Gamma_l(I_f \rightarrow I_i)}{\Gamma_{\text{Weisskopf}}} = \left(Z \frac{l+3}{3} \right)^2 \left(\frac{R}{R_w} \right)^{2l} \beta_l(I_i, I_f), \quad (17)$$

³⁴ A. Bohr and B. R. Mottleson, Kgl. Danske Videnskab. Selskab, Mat.-fys. Medd. 27, No. 16 (1953).

³⁵ V. F. Weisskopf, Phys. Rev. 83, 1073 (1951).

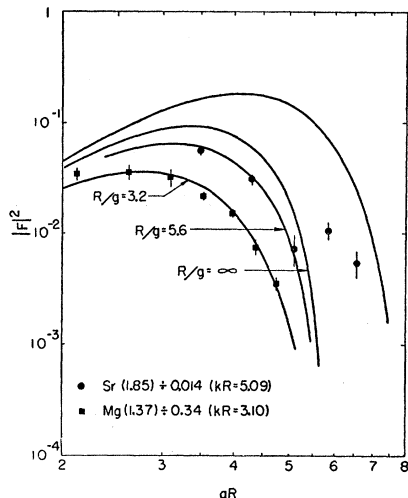


FIG. 6. Comparison of typical experimental and calculated squared inelastic form factors. Both the Sr (1.85 Mev) and Mg (1.37 Mev) are known to be $2+$ levels. The calculated curves are for a "smeared δ -function" transition charge density (see Sec. V) with values of R/g taken from the elastic results. The abscissae for the experimental data are scaled by values of R taken from the elastic results [Table III (a)]. Shown for comparison (upper curve) is a squared form factor calculated from a quadrupole transition charge density whose radial dependence is constant for $r < R$, zero for $r > R$. This would give a poorer fit to the data than the δ -function distribution, indicating that the quadrupole vibrational mode is approximated better by a transverse wave in an incompressible nuclear fluid than by some sort of compressional body wave.

where the numerator of the first quotient is the inelastic cross section, as extrapolated to the forward direction, from the present type of experiment. Note that $|M|^2$ is defined in the same way as $|M|^2$ of Wilkinson.³⁶

Since the absolute cross sections are not known with great accuracy (Sec. II), the experimental values of $\beta_l(I_i, I_f)$ are based on a calibration of absolute cross section obtained by fitting the elastic curves to the calculated elastic form-factors. An alternate and very convenient method would be to obtain $\beta_l(I_i, I_f)$ by normalizing the ratio $|f_l^{i,f}|^2 / |F|^2_{\text{elastic}}$ to the experimental ratio of inelastic to obtain elastic scattering; this method is applicable if the measurements go to values of q sufficiently below the first diffraction minimum. Table IV summarizes the inelastic results in terms of the values of $\beta_l(I_i, I_f)$, $\Gamma_l(I_f \rightarrow I_i)$, and other related parameters.

VI. RESULTS—INELASTIC DATA

In addition to the inelastic scattering observed in the present work in $^{12}\text{Mg}^{24}$, $^{14}\text{Si}^{28}$, $^{18}\text{A}^{40}$, and $^{38}\text{Sr}^{88}$, the 4.43-Mev $2+$ and 7.68-Mev $0+$ levels in $^{6}\text{C}^{12}$, reported by Fregeau³⁷ and Hofstadter¹¹ and the 3.73-Mev level in $^{20}\text{Ca}^{40}$, reported by Hahn *et al.*,⁸ will be considered.

³⁶ D. H. Wilkinson, Phil. Mag. (to be published).

³⁷ Through the generosity of Mr. Fregeau, some data on carbon more recent than those of reference 11 are included here.

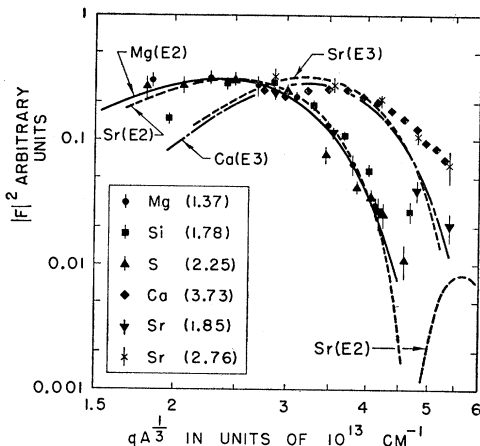


FIG. 7. Inelastic “universal curves.” A composite plot of inelastic data from Mg, Si, S, Ca, and Sr against $qA^{1/3}$. The various form factors are arbitrarily normalized to minimize the spread of points. The point from sulfur and the point from silicon which seem to deviate from the “universal curve” are assumed to contain undetected experimental errors. The curves labeled Mg(E_2), Sr(E_2), Ca(E_3), and Sr(E_3) are calculated for electric-quadrupole and octupole transitions using the “smeared δ -function” transition charge densities of Sec. V, and are arbitrarily normalized.

It is found that when the various experimental form factors are plotted against $qA^{1/3}$ and are arbitrarily normalized together in the region where the form factors are maximum, then practically all the points fall (within experimental accuracy) onto several “universal” curves, (see Fig. 7). Assuming that all the levels observed are electric multipoles,³⁸ then one is tempted to conclude that there is a distinct universal curve for each value of $l=0, 2, 3 \dots$, at least for the lower levels in even-even nuclei. This is partially borne out by what is known about the levels: thus, Mg (1.37 Mev), Si (2.25 Mev), and Sr (1.85 Mev), all of which are known 2+ levels,^{12,14} fall on essentially the same curve; also, Sr (2.76 Mev), which is known¹⁴ to be 3+, gives a distinctly different curve. Carbon, however, seems to be an exception; the data on the 7.68-Mev, 0+ level fit with the Mg-Si-Sr 2+ data about as well as do the carbon 4.43-Mev 2+ data (see Fig. 8). Also, the Mg, Si, and Sr 2+ curves are fitted fairly well by the calculated (smeared δ -function) form factors using R and g from the elastic data, while the carbon curve is not (i.e., carbon 2+ would require a slightly smaller g or larger R).

Undoubtedly, the exact shapes of the form factors are dependent on the details of the actual nuclear wave functions, and it seems plausible that “universal” curves will apply only in nuclei that are heavy enough so that a truly collective model is a good approximation. (It might also be expected that for the shell model the *form*, but not necessarily the magnitude, of the form factor would be the same for all the heavier nuclei.)

³⁸ Most of the observed transitions are known to be electric because of the spins and parities of the levels; also, according to the estimates of Schiff (reference 15) magnetic transitions should be excited with much lower probability.

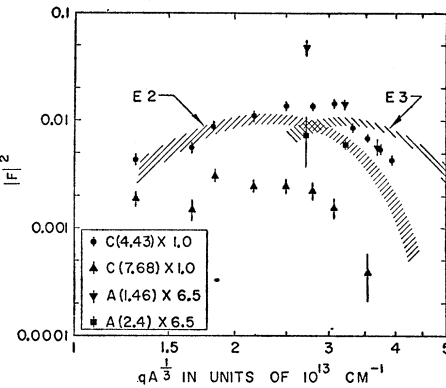


FIG. 8. Comparison of carbon (reference 11) and argon inelastic data to the “universal curves.” The shaded areas, arbitrarily normalized, represent the envelopes of the experimental points of Fig. 7. E_2 refers to quadrupole and E_3 to octupole transitions. It is evident that the known quadrupole cases (4.43 Mev) deviates somewhat from the “universal curve” of the heavier elements, while the C (7.68 Mev) would, if appropriately normalized, fit the “universal curve” almost as well as the 4.43 Mev. The argon data are normalized to make the 2.4 Mev fall on the E_2 curve, although it could equally well fit the E_3 or possibly the monopole curves. The A (1.46 Mev) curve clearly has too steep a slope to fit either the E_2 or E_3 , and therefore is very probably a monopole.

With these considerations in mind, it is felt that some tentative multipolarity assignments still can be made by comparison of the form factors with known cases. The following are considered highly probable³⁹ (refer to Fig. 7):⁴⁰

$$\begin{aligned} &S^{32}(2.25 \text{ Mev}), \quad J=2(+); \\ &Ca^{40}(3.73 \text{ Mev}), \quad J=3(-). \end{aligned}$$

The following are possibilities that need further investigation (Fig. 8):

$$\begin{aligned} &A^{40}(1.46 \text{ Mev}), \quad J=0(+); \\ &A^{40}(2.4 \text{ Mev}), \quad J=2(+). \end{aligned}$$

The quantities β_i (defined in Sec. V), Γ_i , $|M|^2$, and the mean life τ_r for radiative decay to the ground state are listed in Table IV. The transition widths (and mean lives), because of their e^{2l+1} dependence, vary widely; but β_i , which essentially measures the excitation probabilities, is much more uniform from element to element.

The values of $|M|^2$ (based on $R_w = 1.5A^{1/3} \times 10^{-13}$ cm, and with R from Table III) range from ~ 1.8 to ~ 9 ; the results suggest vaguely that the single-particle model is best for nuclei that come just before a magic number (i.e., C and A), and is better for quadrupole than for octupole transitions.

The estimates of the transition widths turn out to be on the order of 0.006 mv for the Sr (2.76 Mev, 3-), to 12.5 mv for the C (4.43 Mev, 2+), corresponding

³⁹ Total angular momentum J [referred to as I_f in Eqs. (11) and (17)] is equivalent to the multipolarity l of the transition by virtue of the 0+ nature of the ground state.

⁴⁰ This was suggested also by Dr. G. Ravenhall and B. Hahn (private communication) from an earlier, cursory examination of the data.

to mean lives for γ decay of 1.08×10^{-10} to 0.53×10^{-13} sec. It seems probable that cases will be found among the $0+ \rightarrow 0+$ transitions and some of the higher multipoles for which the lifetime estimated by this means can be compared to that found directly from the decay of the metastable state. [The 10^{-10} -sec lifetime quoted for Sr probably is not such a case, since the competing $(2.76\text{-Mev}, 3-) \rightarrow (1.85\text{-Mev}, 2+)$, dipole transition would make the actual lifetime much shorter.]

Several partially-resolved levels were seen, especially in sulfur. The data on these are not considered reliable enough to warrant analysis; for example, it appears that the partially resolved 3.8- and 5.8-Mev levels in sulfur could be $2+, 3-,$ or $4+$. Also, two levels not previously reported were seen, one at ~ 6.6 Mev in sulfur and one at ~ 4.3 Mev in strontium. Since it is uncertain that these are not caused by impurities, further investigation is needed to establish this point.

VII. CONCLUSIONS

Within the known limitations of the Born approximation, it has been confirmed that the elastic scattering in the range of Z investigated here can be interpreted fairly well in terms of a nuclear radius and surface thickness. The rms radius is found to vary quite accurately as $A^{\frac{1}{3}}$ for the models used, and the surface thickness is quite constant but may have appreciable variation associated with shell structure. The use of the "folded" charge distribution is suggested as a convenient means of obtaining preliminary estimates of the charge radius and surface-thickness parameters.

Measurement of the inelastic scattering angular

distributions has been shown to be a promising method for investigating the properties of certain excited states, in particular those levels that give rise to electric transitions. Angular momentum assignments are proposed for several levels where this was not known previously, and the transition widths or radiative lifetimes are calculated. It is difficult, in view of the obviously crude transition charge densities used, to estimate the absolute accuracy of these measurements; but except in cases where the J value is in doubt, it seems certain that subsequent work will not alter these answers by as much as an order of magnitude.

ACKNOWLEDGMENTS

The author is greatly indebted to Professor Robert Hofstadter for suggesting this project and for his invaluable help, encouragement, and advice in all phases of the work. Thanks also go to the operating and maintenance crews of the linear accelerator, whose skillful and devoted execution of their duties made the experiments possible; to the members of the electron-scattering group, especially Professor Hofstadter, Dr. J. A. McIntyre, Dr. Beat Hahn, A. W. Knudsen, J. H. Fregeau and R. W. McAllister, for cooperation and material assistance; to B. G. Stuart, of the Stanford University Physics Department, for careful fabrication of the silicon, sulfur, and strontium targets. A special word of appreciation goes to Dr. D. G. Ravenhall for a number of worthwhile discussions, for many suggestions and corrections in the introductory and analytical portions of the manuscript, and for making available formulas from papers which have not yet been published.

Parity Conjugation and Hyperfragments*

S. B. TREIMAN†

Department of Physics, University of Wisconsin, Madison, Wisconsin

(Received August 31, 1956)

The parity conjugation scheme recently proposed by Lee and Yang entails that Λ -hyperfragments should exist as parity doublets, so that a given species of hyperfragment should exhibit two distinct lifetimes, corresponding respectively to the degenerate even- and odd-parity hyperfragment state functions. Likewise there should be two distinct ratios of nonmesonic to mesonic decay. The parity exchange interaction of Λ particles and nucleons, $\Lambda_1 + n \rightleftharpoons \Lambda_2 + n$ (where Λ_1 and Λ_2 are the two members of the Λ particle parity doublet), gives rise to the possibility of interesting interference effects in hyperfragment decay.

INTRODUCTION

IN one of several attempts which have been made to account for the apparent mass degeneracy of θ and τ mesons, Lee and Yang¹ have proposed a scheme of

* Supported by the University of Wisconsin Research Committee by means of funds provided by the Wisconsin Alumni Research Foundation.

† Permanent address: Palmer Physical Laboratory, Princeton University, Princeton, New Jersey.

¹ T. D. Lee and C. N. Yang, Phys. Rev. **102**, 290 (1956).

parity conjugation which runs along the following lines. Particles of odd strangeness² (K, Λ, Σ) are assumed to exist as parity doublets; for given charge there exist two particles of each type, the two members of each doublet having the same spin and essentially the same mass but opposite parity. The θ and τ are the two members of the K -meson doublet. The members of the

² M. Gell-Mann, Phys. Rev. **92**, 833 (1953); also M. Gell-Mann (to be published).